Available online at www.sciencedirect.com
SCIENCE DIRECT®
ELSEVIER
Journal of Magnetism and Magnetic Materials 267 (2003) 133–138
journal of magnetism and magnetic materials
www.elsevier.com/locate/jmmm

Magnetic tunneling junctions with permalloy electrodes: a study of barrier, thermal annealing, and interlayer coupling

Xiaoyong Liu[a,*], Cong Ren[a], Lance Ritchie[a], B.D. Schrag[a], Gang Xiao[a], Lai-feng Li[b]

[a] *Physics Department, Brown University, 182 Hope Street, Providence, RI 02912, USA*
[b] *Technical Institute of Physics and Chemistry, Chinese Academy of Sciences, China*

Received 17 July 2002; received in revised form 25 November 2002

Abstract

Magnetic properties of $Ni_{81}Fe_{19}/Al_2O_3/Ni_{81}Fe_{19}$ tunneling junctions are studied for different Al thicknesses and plasma oxidation times. A maximal magnetoresistance of 34% is obtained with Al thickness of 20 Å. Magnetometry reveals large exchange bias fields ($\sim$400 Oe) over a wide range of barrier thicknesses, indicating junctions of high quality. Transport measurements conducted on junctions before and after thermal annealing show a dramatic improvement in barrier quality after annealing. Interlayer coupling fields have been measured as a function of barrier thickness for different oxidation times.

PACS: 75.70.−I; 85.30.Mn; 85.70.Kh

Keywords: Interlayer coupling; Magnetic tunneling junctions (MTJs); Magnetoresistance; Thermal annealing

Due to potential applications as magnetic random access memory and high-density read/write heads, magnetic tunnel junctions (MTJs) have attracted intense attention in the literature [1,2]. In these devices, spin-dependent tunneling leads to a very large magnetoresistance (MR) in the ferromagnet/insulator/ferromagnet multilayer. The electron transport properties are critically dependent on the quality of the tunneling barrier, with Al_2O_3 being the overwhelming choice [1,3]. For researchers attempting to improve the quality of MTJs, maximizing the MR is still an important issue. The MR value depends on the spin polarization of the top and bottom ferromagnetic electrodes and the quality of the Al_2O_3. Fabrication of high-quality junctions requires that the barrier be smooth, free of pinholes, completely oxidized, and have proper stoichiometry. In practice, MR as large as 50–60% at room temperature has been reported for structures with electrodes composed of CoFe [4–5], an alloy with a high spin polarization. However, the magnetic coercivity of CoFe film is sensitive to its thickness. To our knowledge, the largest MR observed using the more common magnetostriction-free permalloy (Py = $Ni_{81}Fe_{19}$) electrodes is only 28%, with a typical Al thickness of $\sim$10 Å. In this paper, we characterize the effects of different Al thicknesses on the properties of $Py/Al_2O_3/Py$ MTJs with

*Corresponding author. Fax: +1-401-863-2024.
E-mail address: xiaoyong_liu@brown.edu (X. Liu).

0304-8853/03/$ - see front matter
doi:10.1016/S0304-8853(03)00298-1

constant oxidation times and explore thermal annealing effects on the quality of junctions. We obtain a maximum MR of 34%.

The junctions were grown using magnetron sputtering (base pressure 2×10^{-8} Torr) with the structure: substrate/Pt(300 Å)/Py(30 Å)/FeMn (130 Å)/Py(60 Å)/Al_2O_3/Py(120 Å)/Al(490 Å). Samples were deposited on Si(1 0 0) substrates covered by SiO_2. Here Py(60 Å), Al_2O_3, Py(120 Å) are the pinned, barrier, and free layers, respectively. The anti-ferromagnetic (AFM) FeMn layer provides the exchange bias of the pinned layer [6]. The selection of Pt/Py as a buffer layer promotes the $\langle 1\,1\,1 \rangle$ texture of the FeMn layer. During sputtering, a field of 120 Oe was applied in-plane to induce an uniaxial anisotropy, hence, an easy axis, of the pinned layer and free layer. The sputtering rate of each layer was calibrated by low-angle X-ray diffraction, and the thickness was thereafter determined by sputtering time. The barrier was formed by oxidizing a thin layer of Al in oxygen plasma of 90 mTorr for 80 s, unless otherwise noted. Plasma oxidation was done by applying RF bias to substrate with the power density of 4 mw/cm^2. After deposition, samples were patterned via optical lithography and ion beam etching. The junctions examined herein were of equal size ($150 \times 100\,\mu m^2$). For purposes of comparison, some samples were further post-pinned by annealing at 160°C for 3 min in a field of 1.6 kOe applied parallel to the easy axis of the pinned layer and cooled in the same field before taking out for measurement.

A cross-sectional transmission electron microscopy (TEM) study was conducted to illustrate the interfacial structure of junctions before and after post-pinning. While the as-deposited sample has smeared interfaces between layers and a poorly defined Al–Ox barrier (Fig. 1(a)), it is apparent that annealed sample has much cleaner interfaces and a sharper barrier as shown in Fig. 1(b). The roughness at the AlO_x–Py interfaces is estimated to be 3–4 Å. There is also a marked improvement in the smoothness of the SiO_2 underlayer. And this is further confirmed by the atomic force microscopy (AFM) scans on the SiO_2 substrate (Fig. 2). According to RMS measurement performed by AFM, the roughness of SiO_2 surface after annealing (Fig. 2(b)) significantly decreased to 1.6 Å, as compared to 2.8 Å of that before annealing process (Fig. 2(a)). It is inferred that the quality of the MTJ layered structure is, in no small part, a result of the flatness of the SiO_2 layer, and is greatly enhanced by post-pinning process.

The magnetic properties of each MTJ were measured by means of a vibrating sample magnetometer. Fig. 3 shows some representative magnetic hysteresis loops of the pre-patterned multilayers for as-deposited and post-pinned samples. Exchange bias fields H_e as high as 400 Oe are consistently observed on samples after pinning, as compared with 50–200 Oe for as-deposited samples. A long plateau can be seen between the two transitions for the post-pinned sample, indicating the quality of the anti-parallel alignment of the free and pinned layers. The observed increase in exchange bias field is probably associated with the topography change upon annealing and field cooling afterwards as shown by TEM/AFM measurements. The improvement in FeMn

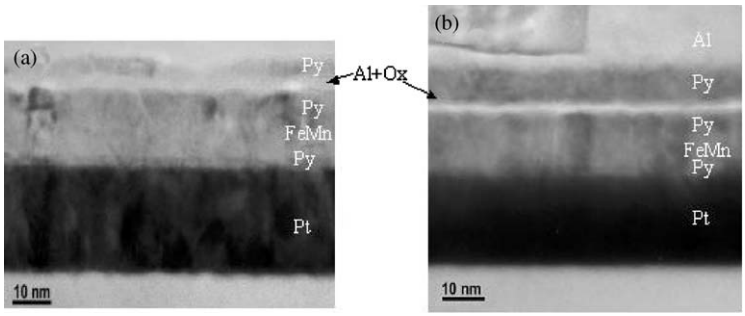

Fig. 1. Cross-sectional TEM images of our MTJs. (a) As-deposited sample, and (b) post-pinned sample.

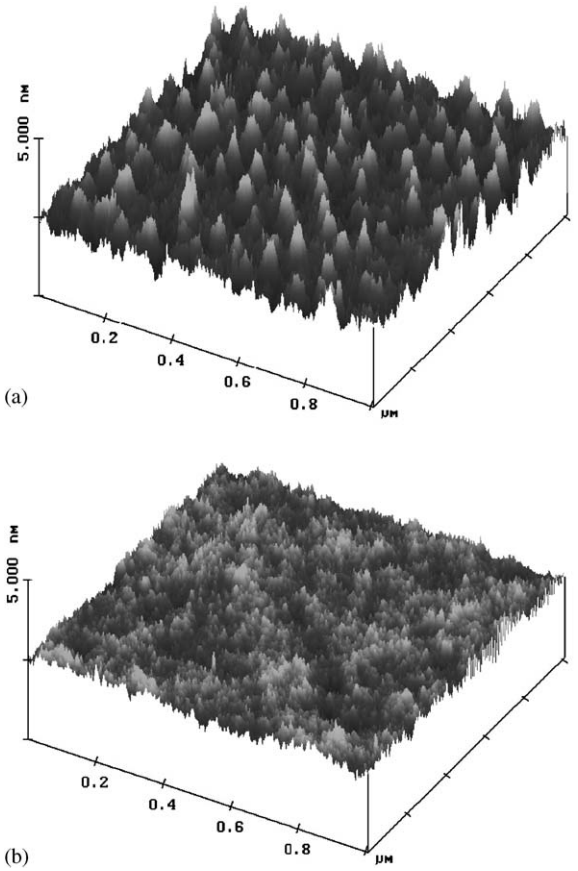

Fig. 2. AFM scans showing the enhanced flatness of SiO_2 substrate for MTJ deposition after post-annealing process. The surface roughness is 2.8 Å for sample before annealing (a), and 1.5 Å for sample after annealing (b).

(1 1 1) texture is also responsible for it. In a related study, we have found that the buffer layer has a strong effect on exchange biasing [7]. It has been previously shown [6] that H_e is inversely proportional to the thickness of the free layer for a given AFM layer. From this result, we have calculated the exchange coupling constant to be ~ 0.25 erg/cm^2 for the post-pinned samples. This value is a little larger than previous reported results [6], it may suggested that upon post-pinning, there are some Mn diffusimg into the NiFe, which effectively reduced the thickness of the pinned layer, and leads to a larger exchange bias field.

Junction transport properties were measured at room temperature (~ 300 K) using a standard

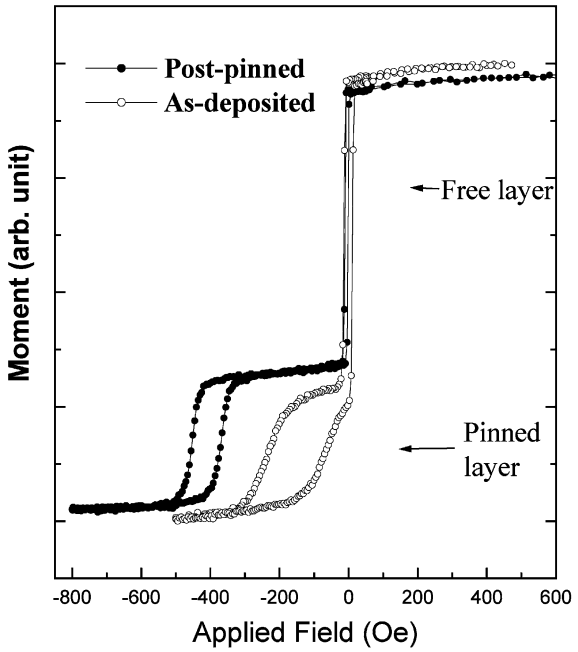

Fig. 3. Hysteresis curves of bulk MTJs for as-deposited (open circles) and post-pinned (solid circles) samples. The two loops corresponding to the switching of the free and pinned layers are shown.

four-point method with a DC bias of 10 mV. A pair of toroidal electromagnets was used to apply DC magnetic fields up to 120 Oe along the easy axis of the sample. This range is far below the exchange bias field (~ 400 Oe); thus, only the switching behavior of top free layer will be considered. The lead resistance ($< 5\,\Omega$) is negligible compared to junction resistance ($> 200\,\Omega$), eliminating anomalous current distribution effects [8]. Typical MR versus field curves for as-deposited and post-pinned junctions with an Al layer thickness of 20 Å are shown in Fig. 4(a). An MR of 34% is achieved for this junction after post-pinning, much larger than that of the as-deposited sample, whose MR is only 12.8%. Measured MR ratios at least doubled after annealing in every junction examined. The larger observed MR value indicates an improvement in junction quality after post-pinning. On the other hand, our measurement showed significant decrease (more than 50%) in junction resistance upon annealing in each case. These results contrast with many previous studies,

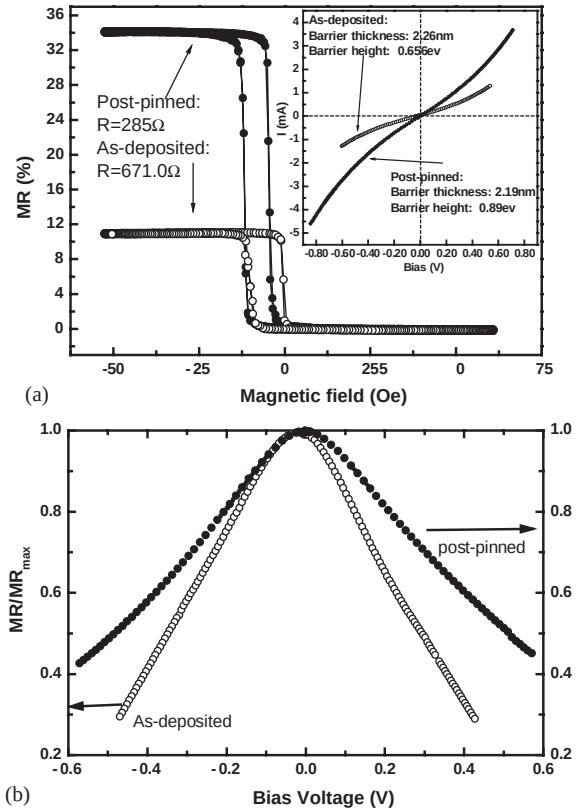

Fig. 4. (a) Typical MR curves of junctions at the optimal Al thickness of 20 Å. The DC voltage bias is 10 mV. Only the switching of the free electrode is displayed in this field range. Inset: $I-V$ curve of same junction. (b) Dependence of MR (normalized to MR ration at zero bias) on bias voltage of the same junction. Open circles and solid circles indicate as-deposited and post-pinned junctions, respectively.

which show increased resistance in proper annealed samples [9].

The $I-V$ characteristics of the same sample were measured in the parallel state (inset of Fig. 4(a)). By fitting to Simmons theory [10], we have extracted effective barrier thicknesses and heights. After annealing, the effective barrier thickness drops from 22.6 to 21.9 Å, while the barrier height increases from 0.66 to 0.89 eV. Other post-pinning effects can also be observed in Fig. 4(a). The coercivity (half of the width of the MR loop) for the post-pinned sample is 3.5 G, smaller than that of the as-deposited sample (5 G). This decrease may be attributed to the decrease in defects after annealing.

Fig. 4(b) gives the bias dependence of MR on the same junction before and after post-pinning. The MR of as-deposited samples falls off more rapidly at higher bias: the bias voltage at which the MR decreases to half of its maximum value is 550 mV for the post-pinned junction, as compared to 300 mV for the as-deposited sample. This indicates that post-pinning greatly improves junction stability. The same behavior can also be seen in other samples with different Al thicknesses. As Sousa and Parkin et al. [4,11] have demonstrated, thermal annealing can improve the quality of junctions and increase the MR ratio. However, this increase is typically on the order of 10–65%, which is less pronounced than our results. For as-deposited junctions, the pinned layer hysteresis loop is not fully separated from the free layer, as seen in Fig. 3. To some extent, this suggests the existence of substantial dispersion of magnetization in the pinned electrode, leading to a sheared loop that crosses the vertical axis, which would decrease the MR value. However after post-pinning, the increased exchange bias creates more uniform anti-parallel alignment between electrodes. In addition, oxygen atoms tend to diffuse more uniformly during pinning, repairing pinholes in the barrier layer. This lead to a larger MR and less wide MR loops compared with post-pinning junctions. Interestingly, as shown in Fig. 4(b), the bias-dependence curve is not symmetric at zero bias for the as-deposited sample; the peak position is shifted slightly toward negative bias. This asymmetry can also be seen in $I-V$ curve as shown in the inset of Fig. 4(a). According to Simmons' theory [10], the potential barrier should be symmetric for our Py/Al_2O_3/Py structures; the asymmetric shape occurred in as-deposited sample is related to partial oxidation of bottom electrode during formation of barrier; it can also be caused by imperfections in the tunnel barrier. For example, local spin-flip scattering in the barrier could cause this asymmetry. Apparently, post-pinning process repairs these defects in some way.

According to Julliere's model [12], $MR = 2P_1P_2/(1-P_1P_2)$, where P_1 and P_2 are the spin polarization of the free and pinned layers, respectively. From this formula, the MR value of 34% for our junctions leads to a spin polarization

of 0.38 for Py. This spin polarization is larger than the accepted value of 0.32 obtained in experiments on ferromagnet–insulator–superconductor junctions [13].

To characterize the effect of barrier thickness on the MR, a series of junctions with different Al thickness (8–26 Å) were grown using identical oxidation times. As shown in Fig. 5(a), each point on the curve in Fig. 5(a) is the average MR of 30 junctions randomly distributed on the wafer, with error bars representing the standard deviation. There is a relatively broad peak in MR corresponding to an optimal nominal Al thickness around 20 Å. The average MR as large as 34% is obtained in this region, which is the highest observed MR as far as we know for the Py/Al_2O_3/Py structure. Outside of this region, MR drops gradually in both directions, corresponding to junctions in which the tunnel barrier is either over- or underoxidized. For junctions with thinner barriers, part of the bottom Py electrode is degraded due to oxidation. Due to the granularity of the Al film, oxidation of the bottom electrode may begin before the Al is fully oxidized. X-ray photoelectron spectroscopy studies have confirmed the existence of Al and oxygen in the bottom electrode of similar structures [14]. PyO_x can serve as a source of spin-flip scattering, which depolarizes the tunnel current, lowering the MR.

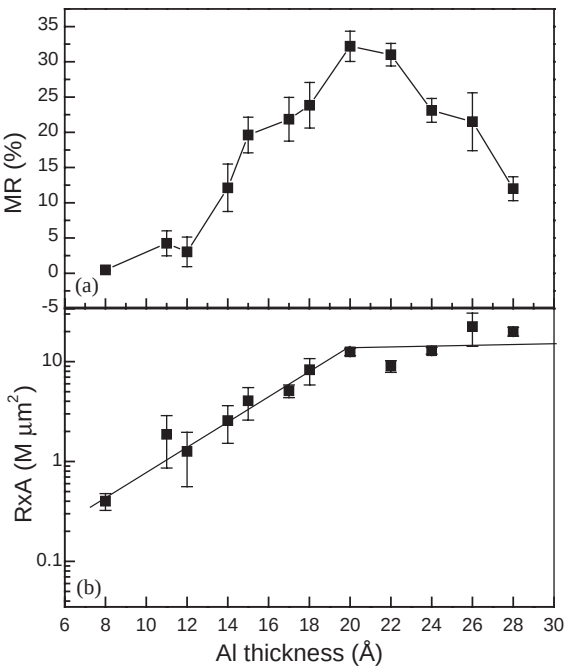

Fig. 5. (a) MR versus Al thickness with constant oxidation time (80 s). Maximum MR of 34% is seen at 20 Å. (b) Semi-log plot of the resistance–area product versus Al thickness. Note the saturation of resistance when Al thickness is greater than 20 Å.

The resistance–area product ($R \times A$) increases exponentially in this range, as displayed in Fig. 5(b), suggesting tunneling-dominated behavior. On the other side of the optimal region, the oxidation time is not sufficient to fully oxidize the Al film, leaving a thin layer of residual metallic Al. The Al_2O_3 layer is roughly constant across this region, and the pure Al underneath barrier has negligible resistance, yielding a flat region in the $R \times A$ curve for thicker Al corresponding to a resistance–area product of $\sim 20\,M\Omega\,\mu m^2$. The optimal 20 Å thickness of Al is much larger than that previously reported (~ 10 Å). One possible reason may be our relatively large junction size, which necessitates a thicker barrier in order to decrease the occurrence of pinholes, which are less likely in micron size junctions. We also studied the oxidation time dependence of MR and resistance, and found it to be less critical than the dependence on Al thickness.

As shown in Fig. 3(a), the free layer MR hysteresis loop is centered at a small negative offset field; this offset is due to interlayer coupling between the free and pinned layers. It is well-known that Néel "orange-peel" coupling, due to interfacial roughness at the two interfaces of the barrier [15], is the dominant mechanism for large junctions. The coupling field is plotted as a function of Al thickness for three different oxidation times in Fig. 6. The offset field H_0 is defined as the midpoint of the left/right switching fields in the free layer hysteresis loop. From Fig. 6, it can be seen that H_0 is maximum at an Al thickness of ~ 14 Å, and decreases monotonically outside of this peak region. It appears that H_0 drops exponentially with thicker Al, as predicted by Néel. In addition, the offset field increases for longer oxidation times, which may be explained by an increased surface roughness of the barrier. Surprisingly, for samples with barriers thinner than 14 Å, H_0 is observed to decrease with

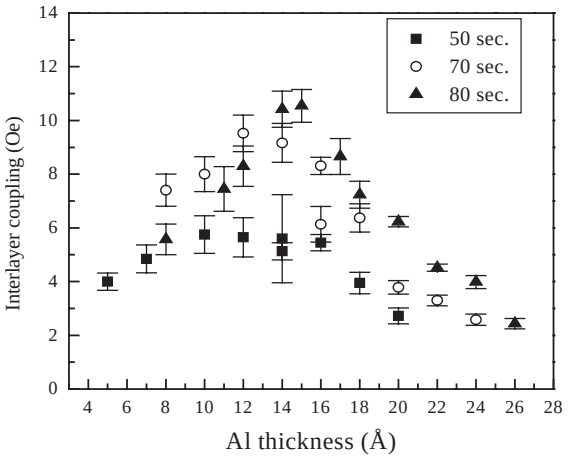

Fig. 6. Interlayer coupling fields (H_0) of tunnel junctions versus Al thickness at different oxidation times. Maximum coupling field is measured with an Al thickness of 14 Å.

decreasing thickness, a result not predicted by the Néel formula. A possible explanation is that the magnetic layer underneath the barrier may be oxidized to some extent, creating an oxide layer of iron or nickel. These compounds are AFM at room temperature, tending to decrease coupling between the top and bottom electrodes. Assuming a constant oxidation time, the thickness of the unwanted layer should increase with decreasing Al thickness, leading to weaker coupling for thinner barriers.

In summary, a series of high-quality Py/Al_2O_3/Py MTJs were fabricated by magnetron sputtering and patterned by photolithography. Cross-sectional images obtained by TEM confirm an improvement in quality of the MTJs after thermal annealing. Exchange bias fields of 450 Oe and MR of up to 34% are obtained with an optimal Al thickness of 20 Å. The obtained value of spin polarization for Py is slightly larger than the accepted value determined by other method. Some unexpected behavior of the interlayer coupling field is observed for junctions with thinner tunnel barriers.

This work was supported by National Science Foundation Grant No. DMR-0071770. Li acknowledges support from the Chinese Academy of Sciences.

References

[1] J.S. Moodera, L.R. Kinder, T.M. Wong, R. Meservey, Phys. Rev. Lett. 74 (1995) 3273.
[2] W.J. Gallagher, S.S.P. Parkin, Yu. Lu, X.P. Bian, A. Marley, K.P. Roche, R.A. Altman, S.A. Rishton, C. Jahnes, T.M. Shaw, G. Xiao, J. Appl. Phys. 69 (1997) 3741.
[3] J.J. Sun, V. Soares, P.P. Fretias, Appl. Phys. Lett. 74 (1999) 448.
[4] Xiu-Feng Han, Mikihiko Oogane, Hitoshi Kubota, Yasuo Ando, Terunobu Miyazaki, Appl. Phys. Lett. 77 (2000) 286.
[5] Masakiyo Tsunoda, Kazuhiro Nishikawa, Satoshi Ogata, Migaky Takashi, Appl. Phys. Lett. 80 (2002) 3135.
[6] J. Nogues, Ivan.K. Schuller, J. Magn. Magn. Mater. 192 (1995) 203.
[7] Lance Ritchie, Xiaoyong Liu, Snorri Ingvarsson, Gang Xiao, Jun Du, John Xiao, J. Magn. Magn. Mater. 247 (2002) 187.
[8] R.J. Vande Veerdonk, J. Nowak, R. Mesevey, J.S. Moodera, W.J.M. de Jone, Appl. Phys. Lett. 71 (1997) 2839.
[9] R.C. Sousa, J.J. Sun, V. Soares, P.P. Freitas, A. Kling, M.F. da Silva, J.C. Soares, Appl. Phys. Lett. 73 (1998) 3288.
[10] J.C. Simmons, J. Appl. Phys. 34 (1963) 1793.
[11] S.S. Parkin, K.P. Roche, M.G. Samant, P.M. Rice, R.B. Beyers, R.E. Scheueriein, E.J. O'sullivan, S.L. Brown, J. Bucchigano, D.W. Abraham, Yu. Lu, M. Rooks, P.L. Trouilloud, R.A. Wanner, W.J. Gallagher, J. Appl. Phys. 85 (1999) 5828.
[12] M. Julliére, Phys. Lett. A 54 (1975) 225.
[13] R. Meservey, P.M. Tedrew, Phys. Rep. 239 (1994) 174.
[14] T. Mitsuzuka, K. Matsuda, H. Tsuge, J. Appl. Phys. 85 (1999) 5807.
[15] L. Neel, CR Acad. Sci. 255 (1962) 1676.